



On-line parameter and state estimation of an air handling unit model: experimental results using the modulating function method

A. Ionesi¹ H. Ramezani² J. Jouffroy³

¹*Danfoss Heating Segment, District Energy, Ulvehavevej 61, DK-7100 Vejle, Denmark. E-mail: ana.ionesi@leanheat.com*

²*SDU Mechatronics, Mads Clausen Institute, University of Southern Denmark, Alsion 2, DK-6400 Sønderborg, Denmark. E-mail: ramezani@mci.sdu.dk*

³*UCL Business and Technology, University College Lillebælt, Seebladsgade 1, DK-5000 Odense C, Denmark. E-mail: jepi@ucl.dk*

Abstract

This paper considers the on-line implementation of the modulating function method, for parameter and state estimation, for the model of an air-handling unit, central element of HVAC systems. After recalling the few elements of the method, more attention is paid on issues related to its on-line implementation, issues for which we use two different techniques. Experimental results are obtained after implementation of the algorithms on a heat flow experiment, and they are compared with conventional techniques (conventional tools from Matlab for parameter estimation, and a simple Luenberger observer for state estimation) for their validation.

Keywords: Modulating function method, heat flow, air-handling unit, parameter and state estimation.

1 Introduction

The challenges of the clear evidence of climate change (Edenhofer and Seyboth, 2013) bring in the front-line new regulations which aim to reduce the green-house gas emissions in all sectors. A notable amount of emissions as well as energy consumption is accounted by buildings, both in the industrial and residential sector. According to Rey-Hernandez et al. (2018), the need for heating is going to decrease while the cooling demand in buildings is going to increase in the coming decades due to the climate change. In this respect, heating ventilation and air conditioning (HVAC) systems with higher energy efficiency and better building designs are continuously researched and developed.

To facilitate the transition towards reducing the en-

ergy consumption and the green-house gas emissions, mathematical models of buildings have been intensively used. The simulation tools available today (Crawley et al., 2008) and the ongoing research offer a high variety of possibilities when it comes to design optimization (Kheiri, 2018), renewable integration (Zhou, 2018), retrofitting (Fan and Xia, 2018), on-line fault detection diagnosis (Bonvini et al., 2014) and even optimized real-time control.

The HVAC system is one very important part of the building, which in Europe is estimated to share 76% of the total energy use (Gruber et al., 2014). The duty of this system is to ensure a comfortable indoor environment by regulating the temperature and the air quality. The well-functioning of the HVAC system will also contribute to an optimal energy consumption. Several

subsystems are considered when modeling an HVAC system, as explained in [Satyavada and Baldi \(2016\)](#). Among them, the air handling unit (AHU) is the subsystem whose role is to condition the air circulated through the building. Different models have been proposed in the literature for modeling an AHU: physical models described by partial differential equations used by most of the simulation tools available ([Crawley et al., 2008](#)), transfer functions ([Afroz et al., 2017](#)), data-driven models ([Afram and Janabi-Sharifi, 2014](#)), and hybrid models or reduced-order models (ROM) ([Afram and Janabi-Sharifi, 2015](#)).

The latter lead to many possibilities as they easily link to estimation and control scenarios where real-time capabilities are important. In this paper, we investigate the use of the so-called modulating function method to perform both state and parameter estimation on a continuous-time ROM- based on a simple thermal-electrical analogy ([Fraisie et al., 2002](#)). In comparison with more conventional approaches using discrete-time such as Kalman filtering, performing both state and parameter estimation in continuous-time relates better to the formalism in which the system is originally modeled and ensures the convergence of the estimates to the real values when sampling time approaches zero ([Unbehauen and Rao, 1997](#)). Compared to their discrete-time counterparts estimating either parameters or state components is the necessity of considering time derivatives. The modulating function technique, originally introduced by Shinbrot ([Shinbrot, 1957](#)), allows to circumvent this issue elegantly, with the use of fixed-length time integrals of the measured signals, akin to continuous-time finite impulse response (FIR) filtering. This offers the additional advantages of giving estimates after a fixed and predetermined amount of time, contrary to usual Kalman-based or observer-based methods. Originally proposed towards parameter estimation, the modulating function method was more recently extended to include state estimation ([Liu et al., 2014](#)) ([Jouffroy and Reger, 2015](#)).

Many studies considering the modulating function approach showed satisfactory performance, but mostly in simulations using artificial data ([Jouffroy and Reger, 2015](#)) or sources generated from real profiles ([Asiri et al., 2017](#)). In contrast to that and to the best of our knowledge, not many applications can be found in the literature dealing with experiments done on actual measurements, to the notable exception of [Daniel-Berhe and Unbehauen \(1998\)](#), where Hartley modulating functions are used to estimate the parameters of a thyristor driven DC-motor.

This paper addresses the question of real-time deterministic parameter and state estimation of an air

handling unit using the modulating function method. The corresponding algorithms are implemented in Matlab/Simulink on an actual heat flow model and experimental results based on noisy measurements are presented. While the model itself is easy to develop and implement, performing estimation of its parameters and states is still a challenge given the actual distributed nature of these parameters, which are also subject to possible changes over time. We also look at practical aspects related to implementation issues for using the modulating function method in an on-line situation, and which we believe has been less considered in the literature. The main contributions of this paper are: 1) the proposal of a technique within the modulating function framework whereby a modulating function is defined based on online measurements as opposed to a priori; 2) another technique where a modulating function is defined as a solution of a state-space representation, thus allowing for rapid implementation in Matlab/Simulink; and 3) the actual implementation and testing of these algorithms on an experimental platform consisting of a heat flow model. In doing so and contrary to what can be usually seen in the literature, we focus more on application aspects than performance and statistical properties of the estimates, which have been done elsewhere (see for example the interesting work in [Liu and Laleg-Kirati \(2015\)](#)). Preliminary results were reported in [Ionesi and Jouffroy \(2018\)](#), where only parameter estimation using the first technique is addressed.

After this introduction, we start this paper by briefly explaining the principle of an HVAC system and that of an AHU, and give a simple ROM of the latter (section 2). Then, the basics of the modulating function method are recalled for both parameter and the state estimation in a state-space context (section 3). A following section is more specifically addressed to issues that are more prone to arise in an on-line scenario, i.e. possible singularities coming from the choice of the modulating function, and ease of implementation of the moving-horizon version in a block diagram environment such as Simulink. For this, we use two different techniques, each one dedicated to these two specific issues (section 4). We validate the proposed techniques on a heat flow model and discuss our experimental results (section 5). Brief concluding remarks end this paper (section 6).

2 Heat Flow Model of an AHU

2.1 System description

The HVAC system within a building can be configured in many different ways with regards to the buildings'

layout and purpose, application or users' needs. It usually contains a variety of components such as chillers, cooling towers, condensing boilers, AHUs, heat pumps, heat recovery units, fans, control valves, pipes, etc. as described, for example, in [Satyavada and Baldi \(2016\)](#). The air flow in a typical compact HVAC system can be represented by the schematic diagram shown in Fig. 1. The heating and cooling coils are part of separate networks with complex units that deliver cold or heat based on requirements. Similar representations can be seen in [Dey and Dong \(2016\)](#) or [Chen and Treado \(2014\)](#).

An important component of the HVAC system is the AHU (marked with green dashed box in Fig. 1). The role of this component is to condition the air that is used for the ventilation of the rooms in order to maintain a comfortable indoor environment in terms of temperature and air quality. In this unit, the fresh air is mixed with air coming from the rooms in a mixing chamber, then is circulated by a constant air volume flow fan over a cooling/heating coil. Based on the needs, the air is heated or cooled accordingly, so that the temperature at the exit of the unit achieves prescribed values.

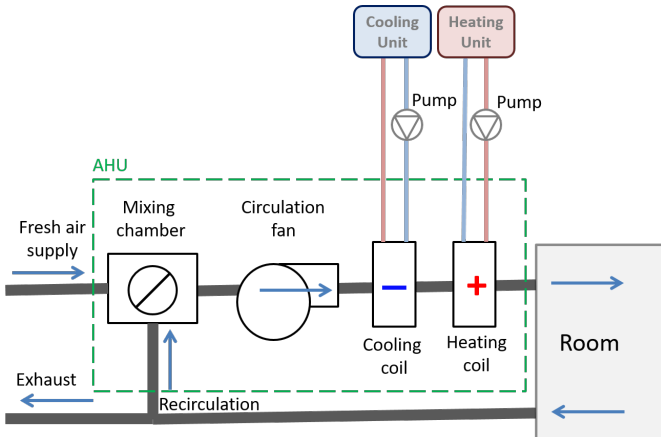


Figure 1: Air flow diagram through a typical fan coil compact HVAC

2.2 Mathematical modeling

Many models have been developed to represent the dynamic heat flow behavior of an AHU. In the existing literature, the models that have been developed range from the use of basic physics ([Setayesh et al., 2015](#)) to advanced data mining algorithms such as artificial neural networks and other machine learning techniques ([Afram et al., 2018](#)). An overview of the variety of these models can be found in [Afroz et al. \(2017\)](#).

The heat flow which is considered here is schemati-

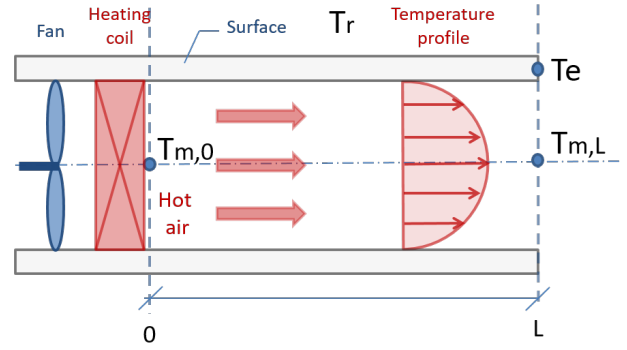


Figure 2: Internal heat flow profile

cally represented in Fig. 2. It simply consists of a fan, a heating coil, and a duct where temperature sensors can be placed. As expected from basic considerations, the temperature profile of the flowing medium, as well as the heat transfer coefficients typically varies with the length L of the duct (see for example [Bergman and Incropera \(2011\)](#)). However, in the present application, only the temperature at the exit of the unit is of interest as it is typically the one which one wants to regulate. Hence we will, in the following, consider the measured temperature $T_{m,L}$, hereafter simply shortened as T_m . In order to model this heat flow, we resort to second-order linear ROM. A similar albeit first-order model is described in [Afram and Janabi-Sharifi \(2015\)](#).

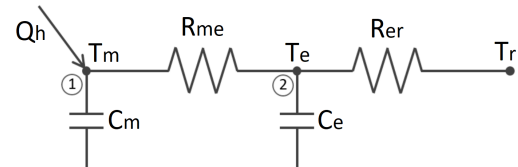


Figure 3: RC network analogy of the heat flow

The proposed 2nd order linear model uses the resistance capacitor (RC) network analogy depicted in Fig. 3. In order to develop the model, we first write a flow balance equation for each node. Hence, we get

$$C_m \frac{dT_m}{dt} = \frac{1}{R_{me}} (T_e - T_m) + Q_h \quad (1)$$

for node 1, representing the air inside the unit, where T_m is the measured temperature in the AHU and T_e is the envelope/surface temperature of the AHU, while Q_h is the heating/cooling load added in the AHU. The constant parameters of this flow balance equation are C_m , the summed heat capacity of the sensor and of the air inside the unit and R_{me} , the thermal resistance

between the temperature sensor and the envelope of the unit.

For node 2, the surface/envelope of the unit, we have the differential relation

$$C_e \frac{dT_e}{dt} = \frac{1}{R_{me}}(T_m - T_e) + \frac{1}{R_{er}}(T_r - T_e) \quad (2)$$

where T_r is the temperature of the room surrounding the unit. In equation (2), constant parameters are C_e , the heat capacity of the envelope of the AHU, and R_{er} , the total thermal resistance between the envelope of the unit and the room.

From eqs. (1)-(2), it is simple to obtain the state-space representation

$$\dot{\mathbf{x}} = \mathbf{A}\mathbf{x} + \mathbf{B}\mathbf{u} \quad (3)$$

$$y = \mathbf{C}\mathbf{x} \quad (4)$$

where, defining the state vector and the input vector as

$$\mathbf{x} = [T_m, T_e]^T, \quad (5)$$

and

$$\mathbf{u} = [Q_h, T_r]^T \quad (6)$$

while assuming we only measure the temperature at the end of the unit, i.e. $y = T_m$, we have the matrices

$$\mathbf{A} = \begin{bmatrix} -\frac{1}{C_m R_{me}} & \frac{1}{C_m R_{me}} \\ \frac{1}{C_e R_{me}} & -\left(\frac{1}{C_e R_{me}} + \frac{1}{C_e R_{er}}\right) \end{bmatrix}, \quad (7)$$

$$\mathbf{B} = \begin{bmatrix} \frac{1}{C_m} & 0 \\ 0 & \frac{1}{C_e R_{er}} \end{bmatrix}, \quad (8)$$

$$\mathbf{C} = [1 \quad 0]. \quad (9)$$

3 The Modulating Function Method: parameter and state estimation

In this section, we briefly recall the basics of the modulating function method. For the sake of clarity, we do so on single-input single-output systems, with the multiple-input case as a direct extension.

The modulating function method being primarily based on an input-output description of a dynamical system, we start, as a preliminary by transforming our state-space presentation (3)-(4). Hence, considering the n -dimensional case where $\mathbf{x} \in \mathbb{R}^n$, $u \in \mathbb{R}$ and $y \in \mathbb{R}$, we differentiate the output equation (4) $n-1$ times and get the well-known expression

$$\bar{\mathbf{y}} = \mathbb{O}\mathbf{x} + \mathbf{T}\bar{\mathbf{u}} \quad (10)$$

where $\bar{\mathbf{y}} = [y, \dot{y}, \dots, y^{(n-1)}]^T$ and $\bar{\mathbf{u}} = [u, \dot{u}, \dots, u^{(n-1)}]^T$. Matrix \mathbb{O} is the well-known observability matrix of the

Kalman criterion and matrix \mathbf{T} is the system specific Toeplitz matrix given by

$$\mathbf{T} = \begin{bmatrix} \mathbf{0} & \mathbf{0} & \dots & \mathbf{0} \\ \mathbf{C}\mathbf{B} & \mathbf{0} & \ddots & \vdots \\ \vdots & \vdots & \ddots & \mathbf{0} \\ \mathbf{C}\mathbf{A}^{n-2}\mathbf{B} & \mathbf{C}\mathbf{A}^{n-3}\mathbf{B} & \dots & \mathbf{0} \end{bmatrix}. \quad (11)$$

Then, differentiating equation (4) one more time and isolating \mathbf{x} in expression (10), we get

$$y^{(n)} = \mathbf{C}\mathbf{A}^n\mathbb{O}^{-1}(\bar{\mathbf{y}} - \mathbf{T}\bar{\mathbf{u}}) + \mathbf{C}\mathbf{C}^R\bar{\mathbf{u}} \quad (12)$$

where the reversed controllability matrix \mathbf{C}^R is given by

$$\mathbf{C}^R = [\mathbf{A}^{(n-1)}\mathbf{B}, \mathbf{A}^{(n-2)}\mathbf{B}, \dots, \mathbf{A}\mathbf{B}, \mathbf{B}]. \quad (13)$$

Note that an obvious condition for expression (12) to be defined is the observability of state-space representation (3)-(4). We thus have the input-output form

$$y^{(n)} = -\mathbf{a}^T\bar{\mathbf{y}} + \mathbf{b}^T\bar{\mathbf{u}} \quad (14)$$

where $\mathbf{a}^T = \mathbf{C}\mathbf{A}^n\mathbb{O}^{-1} = [a_0, a_1, \dots, a_{n-1}]$ and $\mathbf{b}^T = \mathbf{C}\mathbf{C}^R - \mathbf{C}\mathbf{A}^n\mathbb{O}^{-1}\mathbf{T} = [b_0, b_1, \dots, b_{n-1}]$. Defining then the vector \mathbf{Y} as $\mathbf{Y} = [\bar{\mathbf{y}}^T, \bar{\mathbf{u}}^T]^T$, the following parametric form is obtained

$$y^{(n)} = \mathbf{Y}^T\boldsymbol{\theta}, \quad (15)$$

where the unknown parameter vector $\boldsymbol{\theta} \in \mathbb{R}^{2n}$ is given by $\boldsymbol{\theta} = [-\mathbf{a}^T, \mathbf{b}^T]^T$. In case a constant and unknown disturbance d is impacting the system's behavior at the same level as the input, expression (15) can be simply modified such that $\mathbf{Y}_d = [1, \mathbf{Y}^T]^T$ replaces \mathbf{Y} and $\boldsymbol{\theta}_d = [d, \boldsymbol{\theta}^T]^T$ replaces $\boldsymbol{\theta}$.

Before proceeding, let us first recall the definition of a modulating function (see Liu et al. (2014), Jouffroy and Reger (2015)).

Definition 1 *The sufficiently smooth function $\varphi : [0, T] \rightarrow \mathbb{R}$ is called a modulating function (of order k) if at least one of its boundaries and its derivatives up to order k equals zero, i.e. if*

$$\varphi^{(i)}(0) \cdot \varphi^{(i)}(T) = 0, i = \overline{0, k-1}. \quad (16)$$

A modulating function where $\varphi^{(i)}(0) = 0$ and $\varphi^{(i)}(T) \neq 0$ (for $i = \overline{0, k-1}$) is called a left modulating function, while a modulating function with $\varphi^{(i)}(0) \neq 0$ and $\varphi^{(i)}(T) = 0$ is called a right modulating function. If a modulating function is such that we have $\varphi^{(i)}(0) = \varphi^{(i)}(T) = 0$, then it is called a total modulating function.

Note that a more general definition of a modulating function (see [Jouffroy and Reger \(2015\)](#)) allows to include expanding horizons, allowing thus to include alternative integral approaches ([Mathew and Fairman, 1972](#)) ([Saha and Rao, 1980](#)).

In this paper, we are interested in on-line estimation. Regarding parameter estimation, we hereby use the following receding-horizon integral operator on the signal $y(t)$, using a total modulating function given by ([Noack et al., 2018](#))

$$L^i[y] := \int_{t-T}^t (-1)^i \varphi^{(i)}(\tau - t + T) y(\tau) d\tau. \quad (17)$$

where $i = \overline{0, k-1}$ and $T > 0$. Due to the fact that $\varphi(t)$ is a total modulating function and by simple integration by parts, operator (17) has the important property that

$$L^0[y^{(i)}] = L^i[y]. \quad (18)$$

Then, applying operator $L^0[\cdot]$ on each time-varying signal of equality (15), and using property (18), we are able to avoid both explicit time-derivatives of measured signals and unknown initial conditions to get

$$z = \mathbf{w}^T \boldsymbol{\theta}, \quad (19)$$

where

$$z = L^n[y] \quad (20)$$

and

$$\mathbf{w} = [L^0[y], L^1[y], \dots, L^{n-1}[y], L^0[u], L^1[u], \dots, L^{n-1}[u]]^T. \quad (21)$$

Finally, we can obtain an estimate of parameter vector $\boldsymbol{\theta}$ by either proceeding to a conventional receding-horizon Gramian-based estimator ([Reger and Jouffroy, 2009](#)), ([Reger and Jouffroy, 2008](#)) over a horizon $T' > 0$, or aggregate a sufficient number of expressions (19), each one obtained with a different total modulating function, so that with $m_t \geq 2n$ total modulating functions, we get the set of linear equations

$$\mathbf{z} = \mathbf{W}^T \boldsymbol{\theta} \quad (22)$$

where $\mathbf{z} = [z_1, z_2, \dots, z_{m_t}]^T$ and $\mathbf{W} = [\mathbf{w}_1, \mathbf{w}_2, \dots, \mathbf{w}_{m_t}]$. In this case, we can in principle directly get the parameter vector estimate by computing

$$\hat{\boldsymbol{\theta}} = (\mathbf{W}\mathbf{W}^T)^{-1} \mathbf{W}\mathbf{z} \quad (23)$$

or, alternatively, proceed by adding another receding-horizon stage similar to the Gramian-based estimator alluded to in order to remove noise further, and define the estimate as

$$\hat{\boldsymbol{\theta}} = \left(\int_{t-T'}^t \mathbf{W}(\tau) \mathbf{W}^T(\tau) d\tau \right)^{-1} \int_{t-T'}^t \mathbf{W}(\tau) \mathbf{z}(\tau) d\tau. \quad (24)$$

Turning now to state estimation, we resort to an integral operator based, this time, on a left modulating function, and given by

$$L_l^i[y] := \int_{t-T}^t (-1)^i \varphi_l^{(i)}(\tau - t + T) y(\tau) d\tau, \quad (25)$$

where $\varphi_l(t) \in [0, T]$ is a left modulating function. Using again integration by parts, and because of the fact that $\varphi_l(T) \neq 0$, we have

$$L_l^0[y^{(i)}] = \sum_{k=0}^{i-1} (-1)^k \varphi_l^{(k)}(T) y^{(i-1-k)}(t) + L_l^i[y]. \quad (26)$$

Proceeding then by applying operator $L_l^0[\cdot]$ on each signal of equation (14), we get the expression

$$\boldsymbol{\varphi}_l \bar{\mathbf{y}} + \mathbf{a}^T \boldsymbol{\Gamma}_l \bar{\mathbf{y}} - \mathbf{b}^T \boldsymbol{\Gamma}_l \bar{\mathbf{u}} = \mathbf{b}^T \mathbf{L}_l[u] - \mathbf{a}^T \mathbf{L}_l[y] - L_l^n[y] \quad (27)$$

where

$$\boldsymbol{\varphi}_l = \left[(-1)^{n-1} \varphi_l^{(n-1)}(T), (-1)^{n-2} \varphi_l^{(n-2)}(T), \dots, (-1)^0 \varphi_l^{(0)}(T) \right], \quad (28)$$

$$\boldsymbol{\Gamma}_l = \begin{bmatrix} 0 & 0 & \dots & 0 \\ (-1)^0 \varphi_l^{(0)}(T) & 0 & \ddots & \vdots \\ \vdots & \ddots & \ddots & 0 \\ (-1)^{n-2} \varphi_l^{(0)}(T) & \dots & (-1)^0 \varphi_l^{(0)}(T) & 0 \end{bmatrix} \quad (29)$$

and

$$\mathbf{L}_l[y] = [L_l^0[y], L_l^1[y], \dots, L_l^{n-1}[y]]^T \quad (30)$$

(and similarly for $\mathbf{L}_l[u]$).

Noticing then that

$$(\boldsymbol{\varphi}_l + \mathbf{a}^T \boldsymbol{\Gamma}_l) \mathbf{T} = \mathbf{b}^T \boldsymbol{\Gamma}_l, \quad (31)$$

expression (27) can be put into a form similar to linear parametric form (19), i.e. we have

$$z_l = \mathbf{w}_l^T (\bar{\mathbf{y}} - \mathbf{T}\bar{\mathbf{u}}), \quad (32)$$

where

$$z_l = \mathbf{b}^T \mathbf{L}_l[u] - \mathbf{a}^T \mathbf{L}_l[y] - L_l^n[y] \quad (33)$$

and

$$\mathbf{w}_l = (\boldsymbol{\varphi}_l + \mathbf{a}^T \boldsymbol{\Gamma}_l)^T. \quad (34)$$

Combining then $m_l \geq n$ left modulating functions, we obtain, similarly to parametric form (22), the expression

$$\mathbf{z}_l = \mathbf{W}_l^T (\bar{\mathbf{y}} - \mathbf{T}\bar{\mathbf{u}}), \quad (35)$$

which, defining the state corresponding to an observability canonical form as

$$\bar{\mathbf{x}} = \bar{\mathbf{y}} - \mathbf{T}\bar{\mathbf{u}}, \quad (36)$$

leads to its estimate $\hat{\mathbf{x}}$ with an expression similar to estimate (23). Alternatively, we can also estimate the original state of the system (3)-(4) by using expression (10), thus leading to the simple transformation

$$\hat{\mathbf{x}} = \mathbb{O}^{-1}\hat{\mathbf{x}}. \quad (37)$$

4 Implementing the modulating function method for on-line applications

4.1 Using time-varying modulating functions

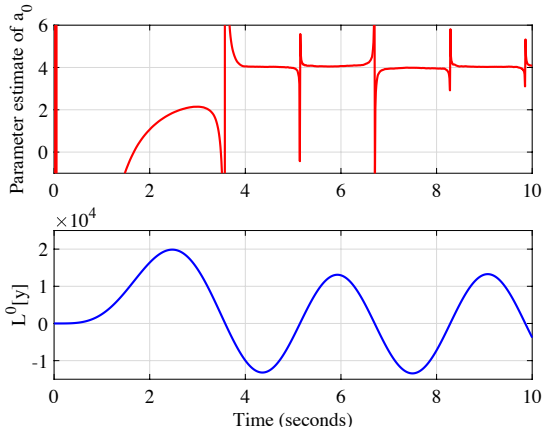


Figure 4: Parameter estimate \hat{a}_0 (top) and operator $L^0[y]$ (bottom) for the oscillator example (38).

Early works on the use of the modulating function method for offline identification of unknown parameters (see for example Pearson and Lee (1985)) start with the definition of a set of specific and predefined modulating functions, which can take different forms (ie Hartly, splines, trigonometric functions, etc). Once a sufficient number of modulating functions are used, one can get a parameter estimate directly by simple inversion, as in (22). However, when considering an on-line and receding-horizon situation, this can generally lead, especially with the presence of noise on the measurements, to singularity issues. For example, considering the trivial system

$$\ddot{y} + a_0 y = 0, \quad (38)$$

applying the modulating function method would simply lead to

$$\hat{a}_0 = -\frac{L^2[y]}{L^0[y]}, \quad (39)$$

where the denominator of (39) could create difficulties. As an illustration, we have simulated the sinusoidal signal $y(t) = 15 \sin 2t$, corrupted with a uniform noise. As can be seen in Fig. 4, the estimate of a_0 , obtained with the fixed total modulating function $\varphi(t) = t^2(t-T)^2$, shows singularities around the time when the signal $L^0[y](t)$ has its zero-crossings (see also similar spiking behaviors in Figure 3 of Co and Ungarala (1997)). Seeing $L^0[y](t) = \langle \varphi, y \rangle$ as a dot product between two functions, one has therefore an orthogonality issue between these functions.

While one way to go around this issue typically consists of using a gradient or recursive least-squares algorithm (or even using more modulating functions), another possibility is to continuously redefine the modulating functions based on the current batch of the measured signals $y(t)$ and $u(t)$.

Indeed, setting the number of total modulating functions to $m_t = 2n$, we impose a normalizing constraint represented as

$$\mathbf{W} = \mathbf{I}_{m_t}. \quad (40)$$

In this way, we are simply bypassing the matrix inversion of (22) or (24). Realizing this constraint hence consists of finding the set of m_t modulating functions that will fulfil (40). Since \mathbf{W} is composed of m_t vectors (21), where $L^i[y]$ is given by (17), we have a set of m_t integro-differential equations, where the unknowns are the m_t total modulating functions φ_k 's, which are also constrained at both their boundaries due to their total modulating function nature.

Let us then transform this set of integro-differential equations into integral equations by considering the n -th order derivative of $\varphi(t)$ arising in expression (20), and define the new function $\alpha : [0, T] \rightarrow \mathbb{R}$ as

$$\alpha(t) := \varphi^{(n)}(t). \quad (41)$$

Then, using the anti-derivative notation

$$f^{(-i)}(\tau) := \int_0^\tau \int_0^{\tau_1} \dots \int_0^{\tau_{i-1}} f(\tau_i) d\tau_i d\tau_{i-1} \dots d\tau_1, \quad (42)$$

the right boundaries of the derivatives of a total modulating function $\varphi(t)$ can simply be re-written as

$$\alpha^{(-i)}(T) = 0, \quad i = \overline{1, n}. \quad (43)$$

while the zero left boundary conditions are simply fulfilled thanks to the successive integration of α . Thus, integral operator can now be re-written as

$$L^i[y] := \int_{t-T}^t (-1)^i \alpha^{(i-n)}(\tau - t + T) y(\tau) d\tau, \quad (44)$$

so that \mathbf{w} in (21) only consists of integrals of α . Hence, expression (40) is now a set of integral equations.

Grouping the right boundary conditions (43) similarly, we also get

$$\mathbf{\Gamma} = \mathbf{0}_{n \times m_t}, \quad (45)$$

where $\mathbf{\Gamma} = [\boldsymbol{\alpha}_1, \boldsymbol{\alpha}_2, \dots, \boldsymbol{\alpha}_{m_t}]$, with each vector $\boldsymbol{\alpha}_j$ composed by all boundary conditions (43) for this specific modulating function, i.e. $\boldsymbol{\alpha}_j = [\alpha_j^{(-n)}, \alpha_j^{(-n+1)}, \dots, \alpha_j^{(-1)}]^T$.

Combining finally (40) with (45), we have a system of linear integral equations, which is simple to solve numerically (details of this numerical method are given in Appendix 6). Once a function $\alpha(\cdot)$ is obtained for each instant t , constraint (40) is fulfilled, and Gramian-like expression (24) is simply replaced with

$$\hat{\boldsymbol{\theta}}(t) = \frac{1}{T'} \int_{t-T'}^t \mathbf{z}(\tau) d\tau. \quad (46)$$

As for state estimation, it is also possible to normalize \mathbf{W}_l similarly so that we have the state estimate

$$\hat{\mathbf{x}} = \mathbb{O}^{-1} \mathbf{z}_l. \quad (47)$$

The most notable difference with parameter estimation, is that, since \mathbf{W}_l in (35) does not depend directly on the measured signals, the $m_l = n$ left modulating functions $\varphi_{l,j}(\cdot)$ can be chosen once and for all t . Note that a similar kind of normalization was also mentioned in the context of least-squares observers (see Medvedev (1996)).

4.2 Direct continuous-time implementation

When needing to choose a particular estimation method, one can obviously focus on performance in terms of the best possible match between the output of the considered plant and its corresponding predicted output using the parameter estimates. However, other factors can also be under consideration, such as ease of implementation, portability of the code, etc. Regarding the on-line use of modulating functions, the latter are usually first discretized (as they would be in the previous subsection or as in Co and Ungarala (1997) and Noack et al. (2018)). However, modern tools for simulation and control such as Matlab/Simulink allows one to program systems and algorithms directly in a continuous-time setting, thus allowing for the additional advantage of being able to consider non-regular samplings. In this section, we present one way to do that, with in mind direct continuous-time implementation, as opposed to looking primarily at performance. To do so, we first begin by introducing a function $\psi : [0, T] \rightarrow \mathbb{R}$, which we will refer to as *reversed modulating function*, and where $\psi(\cdot)$ is such that

$$\psi(t) := \varphi(T - t) \quad (48)$$

where $\varphi(\cdot)$ is our usual modulating function of the very basic following definition 1. In this case, note that, because of reversal (48), a left reversed modulating function corresponds to a right modulating function, and vice-versa. Then, replace operator (17) with

$$M^i[y] := \int_{t-T}^t \psi^{(i)}(t - \tau) y(\tau) d\tau. \quad (49)$$

The advantage of (49), is that, besides its slightly simpler expression than (17), it is directly put under a usual convolution form. Note, also similarly to (18), we have the property that $M^0[y^{(i)}] = M^i[y]$.

Next, we notice that many modulating functions defined in the literature can be expressed by the solution of a differential equation. For example, the total modulating function $\varphi(t) = t^2(t - T)^2$ used for the trivial system (38) is the solution of differential equation $\varphi^{(5)}(t) = 0$. Hence, we introduce the following state-space representation

$$\dot{\boldsymbol{\chi}} = \mathbf{\Lambda} \boldsymbol{\chi}, \quad \boldsymbol{\chi}(0) = \boldsymbol{\ell} \quad (50)$$

$$\psi = \mathbf{\Sigma} \boldsymbol{\chi} \quad (51)$$

where the state vector $\boldsymbol{\chi} \in \mathbb{R}^{n_\psi}$. Thus, integral operator (49) can easily be rewritten using some advantages of state-space representations. For example, $M^0[y]$ can be rewritten as

$$M^0[y] = \int_{t-T}^t \mathbf{\Sigma} e^{\mathbf{\Lambda}(t-\tau)} \boldsymbol{\ell} y(\tau) d\tau. \quad (52)$$

and similarly for the other $M^i[y]$'s. Defining now the new vector $\boldsymbol{\xi}_y \in \mathbb{R}^{n_\psi}$ as

$$\boldsymbol{\xi}_y := \int_0^t e^{\mathbf{\Lambda}(t-\tau)} \boldsymbol{\ell} y(\tau) d\tau, \quad (53)$$

then it can be shown that

$$M^0[y] = \mathbf{\Sigma} [\boldsymbol{\xi}_y(t) - e^{\mathbf{\Lambda}T} \boldsymbol{\xi}_y(t - T)] \quad (54)$$

where vector $\boldsymbol{\xi}_y(t)$ is obtained as the solution of differential equation

$$\dot{\boldsymbol{\xi}}_y = \mathbf{\Lambda} \boldsymbol{\xi}_y + \boldsymbol{\ell} y. \quad (55)$$

Interestingly, imposing now the additional constraint of stability on system (50)¹ means that filter (54)-(55) can be used to implement $M^0[y]$ in software tools such as Matlab/Simulink without having to proceed to a preliminary discretization (the same is of course valid for $M^0[u]$, with a state vector $\boldsymbol{\xi}_u$). Note that computing $M^i[y]$ is not more difficult, and we would simply have

$$M^i[y] = \mathbf{\Sigma} \mathbf{\Lambda}^i [\boldsymbol{\xi}_y(t) - e^{\mathbf{\Lambda}T} \boldsymbol{\xi}_y(t - T)]. \quad (56)$$

¹Note that this is not the case with the polynomial modulating functions typically used in the literature, such as $\varphi(t) = t^2(t - T)^2$ previously mentioned and used in example (38).

Gathering now the $M^i[y]$ terms similarly to (30), we have

$$\mathbf{M}[y] = \mathbb{O}_{MF} [\boldsymbol{\xi}_y(t) - e^{\Lambda T} \boldsymbol{\xi}_y(t-T)], \quad (57)$$

where

$$\mathbf{M}[y] = [M^0[y], M^1[y], \dots, M^{n-1}[y]]^T \quad (58)$$

and

$$\mathbb{O}_{MF} = [\boldsymbol{\Sigma}^T, (\boldsymbol{\Sigma}\boldsymbol{\Lambda})^T, \dots, (\boldsymbol{\Sigma}\boldsymbol{\Lambda}^{n-1})^T]^T. \quad (59)$$

From there, we end up with regression (19) again, where

$$\mathbf{w} = [\mathbf{M}^T[y], \mathbf{M}^T[u]]^T \quad (60)$$

while z is given by

$$z = M^n[y]. \quad (61)$$

In case one wants to favor speed over precision, it is possible to use a single total (reversed) modulating function and use a Gramian-based expression in order to get the parameter estimate. Another advantage of using expressions such as (52) or (54), where the modulating function is generated by a stable system, is that similar expressions can also be used to obtain the parameter estimates themselves. Indeed, as in [Reger and Jouffroy \(2009\)](#), we can use a generalized Gramian expression where the kernel is generated thanks to a reversed modulating function. Indeed, multiply each term of (19) by $\psi(t-\tau)\mathbf{w}(\tau)$ and integrate to get

$$\int_{t-T}^t \psi(t-\tau)\mathbf{w}(\tau)z(\tau)d\tau = \int_{t-T}^t \psi(t-\tau)\mathbf{w}(\tau)\mathbf{w}^T(\tau)d\tau \boldsymbol{\theta} \quad (62)$$

which can be rewritten as

$$M^0[\mathbf{h}] = M^0[\mathbf{G}]\boldsymbol{\theta} \quad (63)$$

where we have vector $\mathbf{h} = \mathbf{w}z$ and matrix $\mathbf{G} = \mathbf{w}\mathbf{w}^T$. Proceeding in the same manner as we did from expressions (49) to (57), we can define, for $M^0[\mathbf{h}]$, the filter equations

$$\dot{\boldsymbol{\xi}}_{\mathbf{h}} = \underline{\boldsymbol{\Lambda}}\boldsymbol{\xi}_{\mathbf{h}} + \underline{\boldsymbol{\ell}}\mathbf{h} \quad (64)$$

$$M^0[\mathbf{h}] = \underline{\boldsymbol{\Sigma}} [\boldsymbol{\xi}_{\mathbf{h}}(t) - e^{\underline{\boldsymbol{\Lambda}}T} \boldsymbol{\xi}_{\mathbf{h}}(t-T)] \quad (65)$$

where $\boldsymbol{\xi}_{\mathbf{h}} \in \mathbb{R}^{2nn_\psi}$, and where $\underline{\boldsymbol{\Lambda}} = \boldsymbol{\Lambda} \otimes \mathbf{I}_{2n}$, $\underline{\boldsymbol{\ell}} = \boldsymbol{\ell} \otimes \mathbf{I}_{2n}$ and $\underline{\boldsymbol{\Sigma}} = \boldsymbol{\Sigma} \otimes \mathbf{I}_{2n}$ (with \otimes for the Kronecker symbol). For $M^0[\mathbf{G}]$, we have same kind of filter, this time with a matrix differential equation

$$\dot{\boldsymbol{\Xi}}_{\mathbf{G}} = \underline{\boldsymbol{\Lambda}}\boldsymbol{\Xi}_{\mathbf{G}} + \underline{\boldsymbol{\ell}}\mathbf{G} \quad (66)$$

$$M^0[\mathbf{G}] = \underline{\boldsymbol{\Sigma}} [\boldsymbol{\Xi}_{\mathbf{G}}(t) - e^{\underline{\boldsymbol{\Lambda}}T} \boldsymbol{\Xi}_{\mathbf{G}}(t-T)] \quad (67)$$

where $\boldsymbol{\Xi}_{\mathbf{G}} \in \mathbb{R}^{2nn_\psi \times 2n}$. Finally, an estimate of parameter vector $\boldsymbol{\theta}$ is obtained by simple inversion as

$$\hat{\boldsymbol{\theta}} = (M^0[\mathbf{G}])^{-1} M^0[\mathbf{h}]. \quad (68)$$

Interestingly, and moving now to state estimation, the method simply consists in repeating the steps (32) to (37) by taking into account that left modulating integral operators $L_i^i[y]$ and $L_i^i[u]$ are replaced by the right reversed modulating integral operators $M_r^i[y]$ and $M_r^i[u]$, where we have the property

$$M_r^0[y^{(i)}] = \sum_{k=0}^{i-1} \psi_r^{(k)}(0)y^{(i-1-k)}(t) + M_r^i[y] \quad (69)$$

(note, therefore, that steps (60) through (68) are obviously not necessary).

5 Case study

As a case study, a heat flow experimental chamber produced by Quanser company is considered. This plant reproduces the thermodynamics of an Air Handling Unit of an HVAC system. A few technical details related to the experimental set-up will be first introduced, while results of on-line parameter and state estimation and their validation will be presented afterwards.

5.1 Quanser heat flow chamber

The heat flow experiment (Fig. 5) consists of a fiberglass chamber equipped with a fan blowing over an electric heating coil. Both the fan and the heater can be controlled externally with a 0 – 5V input signal. The air temperature inside the box is measured by three temperature sensors positioned equidistantly. Additionally, we make use of the Quanser Q8-USB Data Acquisition Board in order to enable the communication between the computer and the experimental chamber.

5.2 Initial set-up and simulation environment

In the literature, the considered system model for control applications is usually of first order model (with or without time delay) ([Malek et al., 2013](#)), ([Yamada, 2005](#)). However, in practice, a second-order model can have its importance, as the surface does not only represent the envelope/box storing heat but also other components (fans, dampers, filters). In a faulty situation where the box /components inside get overheated and can be damaged, estimating the box temperature can

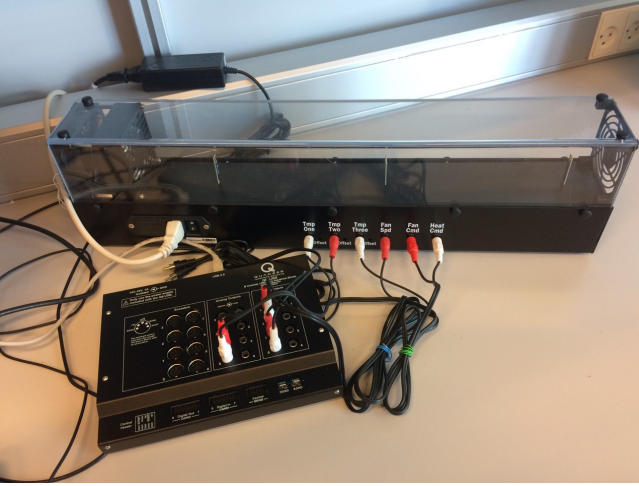


Figure 5: Quanser Heat Flow Experimental setup

generate important information, and help in fault detection. The set-up will be used both for parameter estimation and state estimation scenarios where the latter uses the results of the former. Because the chamber is located in a closed indoor environment and the experiment is conducted on short time interval, we will assume that the room temperature (T_r) is unknown but constant during the experiment. In order to stay close to an actual operation of a constant flow AHU, the fan is operating with a constant speed during the whole experiment.

5.3 On-line parameter estimation

Using steps (10) to (15) on state-space representation (3)-(9), we obtain the ordinary differential equation

$$y^{(2)} = -a_1 y^{(1)} - a_0 y + b_1 u^{(1)} + b_0 u + d \quad (70)$$

where $y(t) = T_m(t)$ is the measured output, $u(t) = 1/k_h Q_h(t)$ is the heater input (with $k_h = 400/120$ W/V being the heater gain), and a_1 , a_0 , b_1 , b_0 and d are the unknown coefficients of the equation, the last one, d , representing the impact of the unknown input T_r mentioned above, and considered here as a constant disturbance. These coefficients are related to the parameters of system (1)-(2) as follows:

$$a_0 = \frac{1}{C_m R_{me} C_e R_{er}} \quad (71)$$

$$a_1 = \frac{1}{C_e R_{me}} + \frac{1}{C_e R_{er}} + \frac{1}{C_m R_{me}} \quad (72)$$

$$b_0 = \frac{1}{C_m C_e R_{me}} + \frac{1}{C_m C_e R_{er}} \quad (73)$$

$$b_1 = \frac{1}{C_m} \quad (74)$$

$$d = \frac{1}{C_m R_{me} C_e R_{er}} T_r. \quad (75)$$

To perform the parameter estimation with the time-varying modulating function technique, we have used the integration period $T = 2000$ sec with a sampling time $T_s = 2$ sec, thus giving a total of 1000 samples. The additional receding horizon interval for obtaining the estimates is $T' = 2000$ sec. For the direct continuous-time implementation technique, the matrices Λ , Σ are simply

$$\Lambda = \begin{bmatrix} 0 & 1 & 0 & 0 & 0 \\ 0 & 0 & 1 & 0 & 0 \\ 0 & 0 & 0 & 1 & 0 \\ 0 & 0 & 0 & 0 & 1 \\ -\lambda^5 & -5\lambda^4 & -10\lambda^3 & -10\lambda^2 & -5\lambda \end{bmatrix} \quad (76)$$

and

$$\Sigma = [1 \ 0 \ \dots \ 0], \quad (77)$$

while the initial conditions of (50), representing the boundary conditions of the modulating function, are set as

$$\ell = \chi(0) = \begin{bmatrix} 0 \\ 0 \\ 2T^2 \\ -12T - 6\lambda T^2 \\ 24 + 48\lambda T + 12\lambda^2 T^2 \end{bmatrix}. \quad (78)$$

To implement filter (54)-(55), we have set $\lambda = 0.02$ (in matrix Λ , see (76), and $\ell = \chi(0)$, see (78)) and $T = 3000$ sec, while for filters (64)-(65) and (66)-(67), we chose $\lambda = 0.001$ and $T = 3000$ sec.

Input profile and persistence of excitation

A key point in parameter estimation is the persistence of excitation of the input signal. Reliable estimates will be obtained if the input signal is sufficiently rich so that the observed response contains the required information to perform the estimation process. As specified in Ljung (1999), if a specific matrix characteristic of the input signal is non-singular, the input is considered to be persistent. It is well-known that, when estimating the parameters of a system with an input signal having enough persistence of excitation, the estimated parameters approach their true values (Khalil, 1996). However, it is worth mentioning that, unfortunately, not enough attention has been given to the consideration of persistent inputs in building models and thus not many studies can be found on this topic (Li and Wen, 2014).

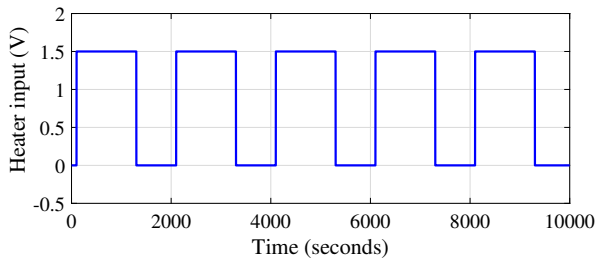


Figure 6: Input profile for parameter estimation

The considered input signal for parameter estimation is a pulse function shown in Fig. 6. This signal is informative enough to capture the dynamics of the heating chamber and obtain the estimates. The amplitude of signal is selected to 1.5V to change the temperature of chamber up to around 30°C. The period of the signal is 2000 sec, with the pulse width of 60%, which is long enough for the plant to reach at least 80% of its final value.

Estimates obtained using the modulating function method

The results of parameter estimation using the modulating function method described in section 3 are presented in Fig. 7. The results are given for both methods: the time-varying modulating function technique (continuous lines) and the direct continuous-time technique (dashed lines). As expected, the direct continuous-time technique, using only one modulating function, does not perform as well as the time-varying technique (although it is computationally more efficient). The latter shows quite good results and converges to an almost constant value after the additional receding horizon interval T' .

Relating to the time-varying modulating function method presented in section 4.1, Fig. 8 shows how one of the total modulating functions (corresponding in this case to a_1) evolves over time. The modulating function is a signal of length $T = 2000$ sec, and the figure shows its evolution from $t = 8000$ sec to $t = 10000$ sec (the curve highlighted in red is the MF at time obtained $t = 8000$ sec). As it can be seen, the amplitude of the MF is constantly adapting to new incoming data/measurements that are fed on-line to the estimator.

5.4 Validation

Since there is no upfront knowledge about the real values of the parameters, we will compare the results of the modulating function method with the results

of two well-known estimation methods available in the System Identification Toolbox for Matlab (Ljung, 2007). These two methods, applicable to continuous-time systems, are the Transfer Function method and the Grey-box estimation method. Moreover, for further inspection of the results, the system output is reconstructed using the estimated parameters compared with the real measurements.

5.4.1 Continuous Transfer Function Estimation

The first method used for comparison is the “tfest” function of Matlab, which estimates a continuous transfer function for the given data. In this method, the input and output of the model are filtered using a pre-filter $L(s)$, and the differential equation of the system is written in a regression form with respect to the filtered signals. The parameters are then estimated to minimize the prediction error.

Matlab uses different numerical search methods to estimate the parameters iteratively. Whenever the default setting is selected, a combination of four line search algorithms ‘Subspace Gauss-Newton least squares search’, ‘Levenberg-Marquardt least squares search’, ‘Adaptive subspace Gauss-Newton search’, and ‘Steepest descent least squares search’ methods will be applied and the first descent direction leading to a reduction in estimation cost is used.

In order to initialize the parameters, different algorithms are available in Matlab. The algorithm used in this study is the instrumental variable approach (Garnier et al., 2003), (Ljung, 2009).

5.4.2 Grey-Box Model Estimation

The second method used for comparison is the grey-box model estimation using the “idgrey” function of Matlab. This method directly uses the parametric state-space representation of the system given in (3)-(4) and minimizes the prediction error.

Matlab uses the same numerical search methods as explained in section 5.4.1. However, contrary to the transfer function estimation technique, the initial value for the parameters should be given by the user.

Table 1 shows the parameters estimated using the MF method together with those obtained by the transfer function and grey-box approaches. As it can be seen, the results of the MF method are very close to the results of the grey-box method, while there is a discrepancy in some parameters with when compared to the transfer function method. The comparison is more clear in Fig. 9 where the output of the estimated models are plotted together and compared with the measured data. The goodness of the fit is 97.57%, 97.33%

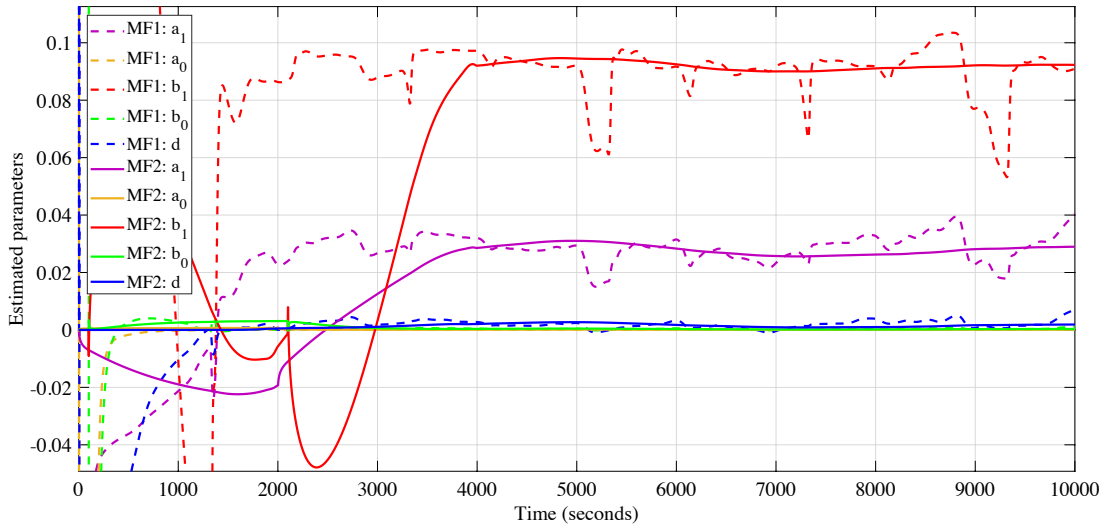


Figure 7: Estimated parameters

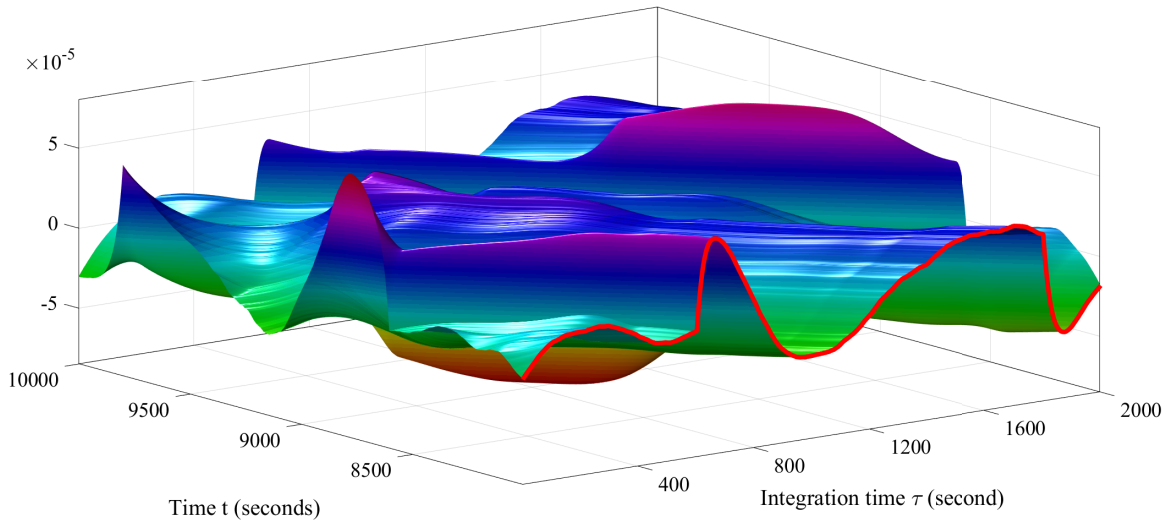


Figure 8: Evolution of the modulation function

and 97.65%, for the modulating function, transfer function and grey-box methods, respectively, which confirms the validity of the proposed MF method.

The main reason for achieving a slightly different (better) result by grey-box estimation method is that the reported goodness of fit was based on non-filtered measured data which matches the structure of grey-box method. The grey-box method works on the original input-output signals whereas the other two methods, i.e. modulating function and transfer function methods, use a pre-filter for the input-output signals ($L(s)$

in transfer function method and the modulating integral operators in the MF method). Therefore the optimization algorithm in the MF and transfer function methods minimizes the filtered error while the reported goodness of fit was based on the original error. In case we would define the goodness of fit based on filtered signals, a higher fit would be achieved for the MF and transfer function methods.

Another important point that should be mentioned is that our implementation of the MF method is on-line while the other two methods are iterative and off-

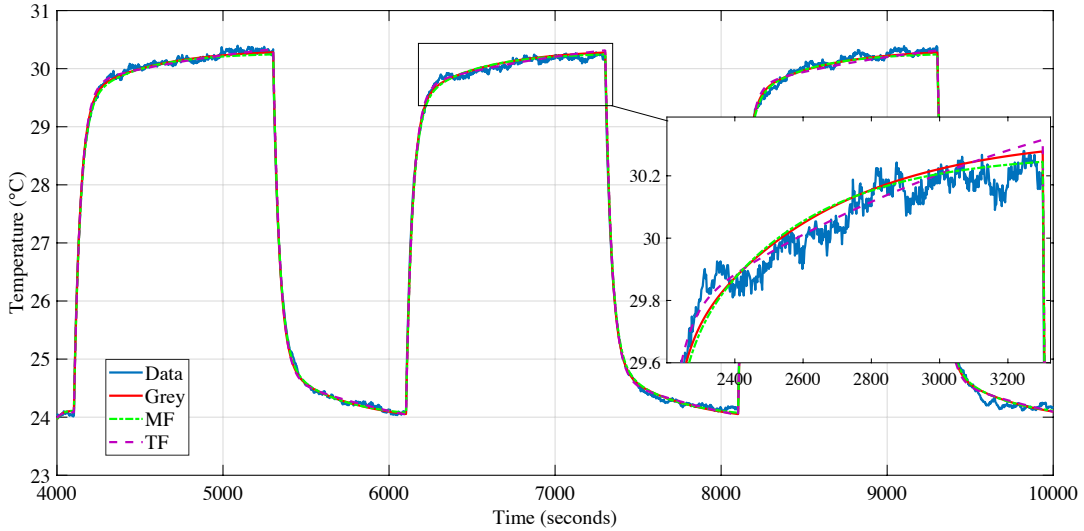


Figure 9: Validation - measured vs. simulated model output

Table 1: Summary of estimated parameters

	Grey-box	Transfer Function	Modulating Function
a_0	6.2415e-05	2.028e-05	7.868e-5
a_1	0.028655	0.02539	0.02896
b_0	2.6766e-04	9.98e-05	3.2983-04
b_1	0.095424	0.09291	0.09228
d	0.001491	4.72991e-04	0.001887

line. In particular, the convergence of the grey-box method highly depends on the initial guess for the parameters (in this study, the estimated parameters from MF method are considered as initial guess for the grey-box method). Therefore, achieving a result in the order of off-line methods in finite time further attests the acceptable performance of our results.

5.5 On-line state estimation

Given the estimated parameters from previous section, it is straightforward to apply the method described in section 3 to obtain the state estimates. Here, both T_m and T_s are estimated on-line using an integration interval $T = 50sec$ with sampling period $T_s = 1sec$.

In a normal operation set-up, the requirements for the temperature at the exit of the AHU might not vary too much in a short time interval. However, to test the proposed state estimation algorithm in different work conditions, a pseudo random input profile shown in Fig. 10 is applied to the system. This is not a common

operating profile, but it helps to visualize the state estimator and evaluate its behavior.

In Fig. 11, it can be observed that the estimated temperature inside the chamber is very close to the noisy measured temperature. Also, as expected, the value for the state representing the envelope temperature of the chamber is lower than the temperature inside, and follows the same heating profile which is in perfect concordance with the heater input profile. The estimated states are comparably good with the ones obtained from a standard observer. In this specific case, the convergence of the states is faster due to the fixed integration interval, which ensures convergence after the first receding horizon window.

6 Conclusion

A 2nd-order model is presented in this paper to represent the heat flow in the air handling unit present in compact HVAC systems. To facilitate the real-time applications of the model, we have proposed the use of a comparably unconventional method, the modulating function, with two different implementation approaches.

As a case study, a heat flow experiment by Quanser, whose thermodynamics are very close to those of an AHU, is considered. The on-line parameter and state estimation algorithms were implemented in Matlab/Simulink. The results underline the potential of this approach, showing a good match between the measured and estimated parameters and states. A good convergence of the parameters was observed, having as

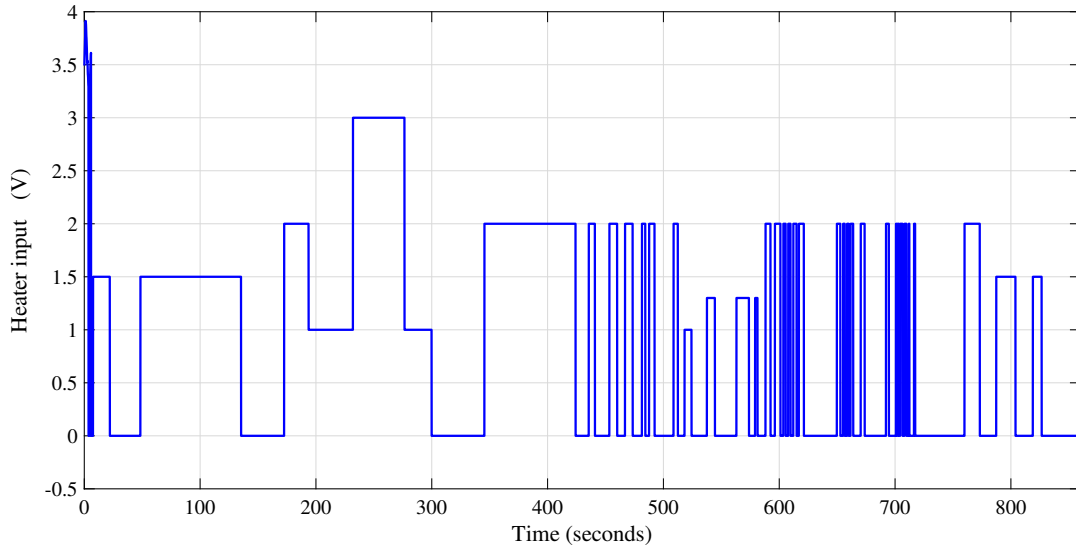


Figure 10: Input profile for state estimation

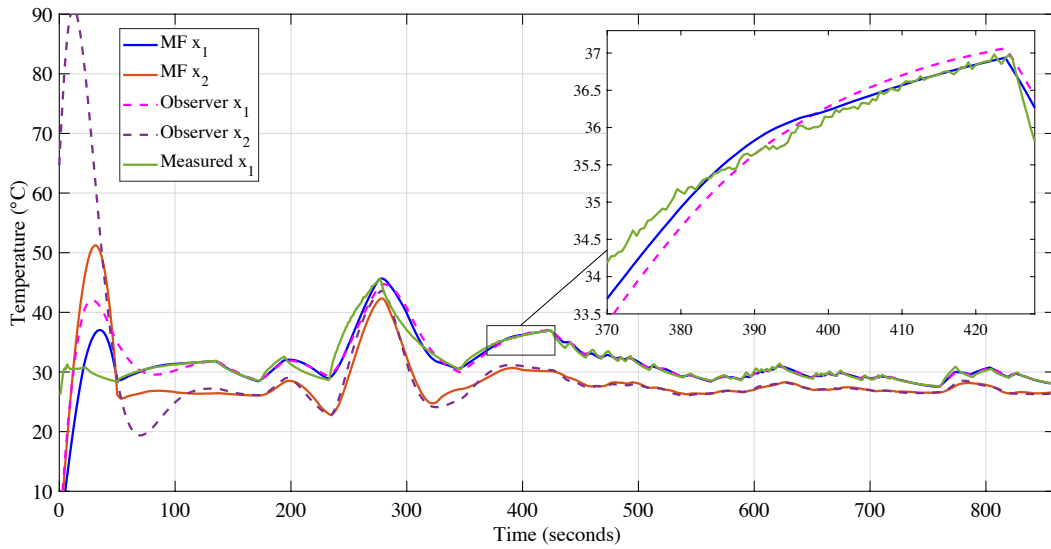


Figure 11: Measured vs. estimated temperature inside the heating chamber using the modulating function and simple observer.

a baseline the parameters estimated with standard estimation methods: the transfer function method and the grey-box method. Moreover, using several (as opposed to only one) modulating functions gives a better estimation of the parameters compared with an approach that uses only one, at the cost of speed although the latter requires less resources to implement and run. The method can be successfully used for on-line state estimation as well, the results showing similar performances to a standard observer.

Acknowledgments

This work was supported by Danfoss, Heating Segment, District Energy Vertical.

Appendix: Numerical integration

For implementing the proposed estimation method a simple Riemann sum is used, taking into account that the signals $y(t)$ and $\mathbf{u}(t)$ are in practice sampled at

regular intervals. Therefore, for the simple boundary condition (43), with $i = 1$, we use the approximation

$$\alpha^{(-1)}(T) = \int_{t-T}^t \alpha(\tau-t+T) d\tau \approx \sum_{k=1}^N T_s \underline{\alpha}(k) = T_s \mathbf{1}^T \underline{\alpha} \quad (79)$$

where N is the number of samples over the interval, T_s is the sampling period, and $\underline{\alpha}(k)$ is the sampled value of function α at iteration k , which gives the vector $\underline{\alpha} = [\underline{\alpha}(1), \underline{\alpha}(2), \dots, \underline{\alpha}(N)]^T$. Vector $\mathbf{1}$ is a vector of dimension N containing only ones. Using a similar reasoning, $\alpha^{(-1)}(\tau)$ can be approximated as

$$\alpha^{(-1)}(\tau) = \int_{t-T}^{\tau} \alpha(\sigma-t+T) d\sigma \approx \sum_{l=1}^k T_s \underline{\alpha}(l) =: \underline{\alpha}^{(-1)}(k) \quad (80)$$

so that

$$\underline{\alpha}^{(-1)} = T_s \mathbf{Q} \underline{\alpha} \quad (81)$$

where $\underline{\alpha}^{(-1)} = [\underline{\alpha}^{(-1)}(1), \underline{\alpha}^{(-1)}(2), \dots, \underline{\alpha}^{(-1)}(N)]^T$, while the matrix \mathbf{Q} is a lower triangular matrix of ones given by

$$\mathbf{Q} = \begin{bmatrix} 1 & 0 & \dots & 0 \\ \vdots & \ddots & \ddots & \vdots \\ 1 & \dots & 1 & 0 \\ 1 & 1 & \dots & 1 \end{bmatrix}. \quad (82)$$

Hence, for $i = 2$, condition (43) gives

$$\alpha^{(-2)}(T) = \int_{t-T}^t \alpha^{(-1)}(\tau-t+T) d\tau \approx T_s^2 \mathbf{1}^T \mathbf{Q} \underline{\alpha}. \quad (83)$$

and for $i = \overline{3}, \overline{n}$:

$$\alpha^{(-i)}(T) = \int_{t-T}^t \alpha^{(-i+1)}(\tau-t+T) d\tau \approx T_s^i \mathbf{1}^T \mathbf{Q}^{i-1} \underline{\alpha}. \quad (84)$$

The operators $L^i[y]$ of \mathbf{w} in equation (44) can be similarly approximated, so that

$$\begin{aligned} L^i[y] &:= \int_{t-T}^t (-1)^i \alpha^{(i-n)}(\tau-t+T) y(\tau) d\tau \\ &\approx (-1)^i T_s^{n-i+1} \underline{\mathbf{y}}^T \mathbf{Q}^{n-i} \underline{\alpha}, \quad i = \overline{0}, \overline{n-1} \end{aligned} \quad (85)$$

Likewise are defined the remaining terms of \mathbf{w} in expression (44), where vector $\underline{\mathbf{y}}$ in operator approximation (85) is replaced by $\underline{\mathbf{u}}$. Taking now $m_t = 2n$ modulating functions, \mathbf{W} in equation (40) can thus be approximated by

$$\mathbf{W} \approx \underline{\mathbf{W}} = \underline{\mathbf{K}} \underline{\alpha} \quad (86)$$

where $\underline{\alpha} = [\underline{\alpha}_1, \underline{\alpha}_2, \dots, \underline{\alpha}_{m_t}]$ and the matrix $\underline{\mathbf{K}}$ is given by

$$\underline{\mathbf{K}} = \begin{bmatrix} (-1)^0 T_s^{n+1} \underline{\mathbf{y}}^T \mathbf{Q}^n \\ \vdots \\ (-1)^{n-1} T_s^2 \underline{\mathbf{y}}^T \mathbf{Q} \\ (-1)^0 T_s^{n+1} \underline{\mathbf{u}}^T \mathbf{Q}^n \\ \vdots \\ (-1)^{n-1} T_s^2 \underline{\mathbf{u}}^T \mathbf{Q} \end{bmatrix}. \quad (87)$$

Proceeding similarly with the discrete approximation of $\mathbf{\Gamma}$ in boundary constraint expression (45), it can be expressed

$$\mathbf{\Gamma} \approx \underline{\mathbf{\Gamma}} = \underline{\mathbf{B}} \underline{\alpha} \quad (88)$$

where

$$\underline{\mathbf{B}} = \begin{bmatrix} T_s^n \mathbf{1}^T \mathbf{Q}^{n-1} \\ \vdots \\ T_s^2 \mathbf{1}^T \mathbf{Q} \\ T_s \mathbf{1}^T \end{bmatrix}. \quad (89)$$

Then, matrix $\underline{\alpha}$ is obtained by simple pseudoinversion, i.e.

$$\underline{\alpha} = \begin{bmatrix} \underline{\mathbf{K}} \\ \underline{\mathbf{B}} \end{bmatrix}^+ \begin{bmatrix} \mathbf{I}_{m_\phi} \\ \mathbf{0}_{n \times m_\phi} \end{bmatrix}. \quad (90)$$

The discrete approximation of \mathbf{z} is given by

$$\mathbf{z} \approx \underline{\mathbf{z}} = T_s \underline{\mathbf{y}}^T \underline{\alpha}. \quad (91)$$

The parameter estimate vector is finally obtained after applying the simple discretized version of receding-horizon expression (46).

References

- Afram, A., Fung, A. S., Janabi-Sharifi, F., and Raahemifar, K. Development and performance comparison of low-order black-box models for a residential hvac system. *Journal of Building Engineering*, 2018. 15:137–155. doi:<https://doi.org/10.1016/j.jobbe.2017.11.021>.
- Afram, A. and Janabi-Sharifi, F. Review of modeling methods for hvac systems. *Applied Thermal Engineering*, 2014. 67(1-2):507–519. doi:<https://doi.org/10.1016/j.applthermaleng.2014.03.055>.
- Afram, A. and Janabi-Sharifi, F. Gray-box modeling and validation of residential hvac system for control system design. *Applied Energy*, 2015. 137:134–150. doi:<https://doi.org/10.1016/j.apenergy.2014.10.026>.
- Afroz, Z., Shafiqullah, G., Urme, T., and Higgins, G. Modeling techniques used in building hvac control systems: A review. *Renewable and Sustainable Energy Reviews*, 2017. doi:<https://doi.org/10.1016/j.rser.2017.10.044>.

- Asiri, S., Elmetennani, S., and Laleg-Kirati, T.-M. Moving-horizon modulating functions-based algorithm for online source estimation in a first-order hyperbolic partial differential equation. *Journal of Solar Energy Engineering*, 2017. 139(6):061007. doi:<https://doi.org/10.1115/1.4037743>.
- Bergman, T. L. and Incropera, F. P. *Fundamentals of heat and mass transfer*. John Wiley & Sons, 2011.
- Bonvini, M., Sohn, M. D., Granderson, J., Wetter, M., and Piette, M. A. Robust on-line fault detection diagnosis for hvac components based on nonlinear state estimation techniques. *Applied Energy*, 2014. 124:156 – 166. doi:<https://doi.org/10.1016/j.apenergy.2014.03.009>.
- Chen, Y. and Treado, S. Development of a simulation platform based on dynamic models for hvac control analysis. *Energy and Buildings*, 2014. 68:376–386. doi:<https://doi.org/10.1016/j.enbuild.2013.09.016>.
- Co, T. B. and Ungarala, S. Batch scheme recursive parameter estimation of continuous-time systems using the modulating functions method. *Automatica*, 1997. 33(6):1185–1191. doi:[https://doi.org/10.1016/S0005-1098\(97\)00020-4](https://doi.org/10.1016/S0005-1098(97)00020-4).
- Crawley, D. B., Hand, J. W., Kummert, M., and Griffith, B. T. Contrasting the capabilities of building energy performance simulation programs. *Building and Environment*, 2008. 43(4):661 – 673. doi:<https://doi.org/10.1016/j.buildenv.2006.10.027>. Part Special: Building Performance Simulation.
- Daniel-Berhe, S. and Unbehauen, H. Experimental physical parameter estimation of a thyristor driven dc-motor using the hmf-method. *Control Engineering Practice*, 1998. 6(5):615–626. doi:[https://doi.org/10.1016/S0967-0661\(98\)00036-7](https://doi.org/10.1016/S0967-0661(98)00036-7).
- Dey, D. and Dong, B. A probabilistic approach to diagnose faults of air handling units in buildings. *Energy and Buildings*, 2016. 130:177 – 187. doi:<https://doi.org/10.1016/j.enbuild.2016.08.017>.
- Edenhofer, O. and Seyboth, K. Intergovernmental panel on climate change (ipcc). In J. F. Shogren, editor, *Encyclopedia of Energy, Natural Resource, and Environmental Economics*, pages 48 – 56. Elsevier, Waltham, 2013. doi:<https://doi.org/10.1016/B978-0-12-375067-9.00128-5>.
- Fan, Y. and Xia, X. Building retrofit optimization models using notch test data considering energy performance certificate compliance. *Applied Energy*, 2018. 228:2140 – 2152. doi:<https://doi.org/10.1016/j.apenergy.2018.07.043>.
- Fraisse, G., Viardot, C., Lafabrie, O., and Achard, G. Development of a simplified and accurate building model based on electrical analogy. *Energy and buildings*, 2002. 34(10):1017–1031. doi:[https://doi.org/10.1016/S0378-7788\(02\)00019-1](https://doi.org/10.1016/S0378-7788(02)00019-1).
- Garnier, H., Mensler, M., and Richard, A. Continuous-time model identification from sampled data: implementation issues and performance evaluation. *International journal of Control*, 2003. 76(13):1337–1357. doi:<https://doi.org/10.1080/0020717031000149636>.
- Gruber, M., Trüschel, A., and Dalenbäck, J.-O. Alternative strategies for supply air temperature control in office buildings. *Energy and Buildings*, 2014. 82:406–415. doi:<https://doi.org/10.1016/j.enbuild.2014.06.056>.
- Ionesi, A. and Jouffroy, J. On-line parameter estimation of an air handling unit model: experimental results using the modulating function method. In *2018 IEEE International Conference on Advanced Intelligent Mechatronics (AIM)*. 2018. doi:[10.1109/AIM.2018.8452284](https://doi.org/10.1109/AIM.2018.8452284).
- Jouffroy, J. and Reger, J. Finite-time simultaneous parameter and state estimation using modulating functions. In *Control Applications (CCA), 2015 IEEE Conference on*. IEEE, pages 394–399, 2015. doi:[10.1109/CCA.2015.7320661](https://doi.org/10.1109/CCA.2015.7320661).
- Khalil, H. K. Adaptive output feedback control of nonlinear systems represented by input-output models. *IEEE Transactions on Automatic Control*, 1996. 41(2):177–188. doi:[10.1109/9.481517](https://doi.org/10.1109/9.481517).
- Kheiri, F. A review on optimization methods applied in energy-efficient building geometry and envelope design. *Renewable and Sustainable Energy Reviews*, 2018. 92:897 – 920. doi:<https://doi.org/10.1016/j.rser.2018.04.080>.
- Li, X. and Wen, J. Review of building energy modeling for control and operation. *Renewable and Sustainable Energy Reviews*, 2014. 37:517–537. doi:<https://doi.org/10.1016/j.rser.2014.05.056>.
- Liu, D.-Y. and Laleg-Kirati, T.-M. Robust fractional order differentiators using generalized modulating functions method. *Signal Processing*, 2015. 107:395–406. doi:<https://doi.org/10.1016/j.sigpro.2014.05.016>.

- Liu, D.-Y., Laleg-Kirati, T.-M., Perruquetti, W., and Gibaru, O. Non-asymptotic state estimation for a class of linear time-varying systems with unknown inputs. In *the 19th World Congress of the International Federation of Automatic Control 2014*. 2014. doi:<https://doi.org/10.3182/20140824-6-ZA-1003.02036>.
- Ljung, L., editor. *System Identification (2Nd Ed.): Theory for the User*. Prentice Hall PTR, Upper Saddle River, NJ, USA, 1999.
- Ljung, L. System identification toolbox for use with {MATLAB}. 2007.
- Ljung, L. *Experiments with identification of continuous time models*. Linköping University Electronic Press, 2009.
- Malek, H., Luo, Y., and Chen, Y. Identification and tuning fractional order proportional integral controllers for time delayed systems with a fractional pole. *Mechatronics*, 2013. 23(7):746 – 754. doi:<https://doi.org/10.1016/j.mechatronics.2013.02.005>.
1. Fractional Order Modeling and Control in Mechatronics 2. Design, control, and software implementation for distributed MEMS (dMEMS).
- Mathew, A. and Fairman, F. Identification in the presence of initial conditions. *IEEE Transactions on Automatic Control*, 1972. 17(3):394–396. doi:[10.1109/TAC.1972.1099997](https://doi.org/10.1109/TAC.1972.1099997).
- Medvedev, A. Continuous least-squares observers with applications. *IEEE Transactions on Automatic Control*, 1996. 41(10):1530–1537. doi:[10.1109/9.539439](https://doi.org/10.1109/9.539439).
- Noack, M., Botha, T., Hamersma, H. A., Ivanov, V., Reger, J., and Els, S. Road profile estimation with modulation function based sensor fusion and series expansion for input reconstruction. In *Advanced Motion Control (AMC), 2018 IEEE 15th International Workshop on*. IEEE, pages 547–552, 2018. doi:[10.1109/AMC.2019.8371152](https://doi.org/10.1109/AMC.2019.8371152).
- Pearson, A. and Lee, F. On the identification of polynomial input-output differential systems. *IEEE Transactions on Automatic Control*, 1985. 30(8):778–782. doi:[10.1109/TAC.1985.1104051](https://doi.org/10.1109/TAC.1985.1104051).
- Reger, J. and Jouffroy, J. Algebraische ableitungsschätzung im kontext der rekonstruierbarkeit (algebraic time-derivative estimation in the context of reconstructibility). *at-Automatisierungstechnik*, 2008. 56(6 (2008)):324–331. doi:<https://doi.org/10.1524/auto.2008.0711>.
- Reger, J. and Jouffroy, J. On algebraic time-derivative estimation and deadbeat state reconstruction. In *Proceedings of the 48th IEEE Conference on Decision and Control (CDC) held jointly with 2009 28th Chinese Control Conference*. pages 1740–1745, 2009. doi:[10.1109/CDC.2009.5400719](https://doi.org/10.1109/CDC.2009.5400719).
- Rey-Hernandez, J. M., Yousif, C., Gatt, D., Velasco-Gomez, E., Jose-Alonso, J. S., and Rey-Martinez, F. J. Modelling the long-term effect of climate change on a zero energy and carbon dioxide building through energy efficiency and renewables. *Energy and Buildings*, 2018. 174:85 – 96. doi:<https://doi.org/10.1016/j.enbuild.2018.06.006>.
- Saha, D. C. and Rao, G. P. Identification of lumped linear systems in the presence of unknown initial conditions via poisson moment functionals. *International Journal of Control*, 1980. 31(4):637–644. doi:<https://doi.org/10.1080/00207178008961071>.
- Satyavada, H. and Baldi, S. An integrated control-oriented modelling for hvac performance benchmarking. *Journal of Building Engineering*, 2016. 6:262–273. doi:<https://doi.org/10.1016/j.jobe.2016.04.005>.
- Setayesh, H., Moradi, H., and Alasty, A. A comparison between the minimum-order & full-order observers in robust control of the air handling units in the presence of uncertainty. *Energy and Buildings*, 2015. 91:115–130. doi:<https://doi.org/10.1016/j.enbuild.2015.01.016>.
- Shinbrot, M. On the analysis of linear and nonlinear systems. *Trans. ASME*, 1957. 79(3):547–552.
- Unbehauen, H. and Rao, P. Identification of continuous-time systems: a tutorial. *IFAC Proceedings Volumes*, 1997. 30(11):973–999. doi:[https://doi.org/10.1016/S1474-6670\(17\)42970-3](https://doi.org/10.1016/S1474-6670(17)42970-3).
- Yamada, K. Modified pid controllers for minimum phase systems and their practical application. In *Proceedings of the Electrical Engineering/Electronics, Computer, Telecommunication and Information Technology (ECTI) International Conference II*. pages 457–460, 2005.
- Zhou, Y. Evaluation of renewable energy utilization efficiency in buildings with exergy analysis. *Applied Thermal Engineering*, 2018. 137:430 – 439. doi:<https://doi.org/10.1016/j.applthermaleng.2018.03.064>.